energies

MDPI

Article

Estimate of Hot Dry Rock Geothermal Resource in Daqing Oilfield, Northeast China

Guangzheng Jiang [1,2], Yi Wang [1,2], Yizuo Shi [1,2], Chao Zhang [1,2], Xiaoyin Tang [3,*] and Shengbiao Hu [1,*]

1 State Key Laboratory of Lithospheric Evolution, Institute of Geology and Geophysics, Chinese Academy of Sciences, Beijing 100029, China; guangzheng@mail.iggcas.ac.cn (G.J.); wangyi@mail.iggcas.ac.cn (Y.W.); ystxb@mst.edu (Y.S.); zhangchao@mail.iggcas.ac.cn (C.Z.)
2 University of Chinese Academy of Sciences, Beijing 100101, China
3 School of Human Settlements and Civil Engineering, Xi'an Jiaotong University, Xi'an 710049, China
* Correspondence: xytang2015@xjtu.edu.cn (X.T.); sbhu@mail.iggcas.ac.cn (S.H.); Tel.: +86-29-8299-8519 (X.T.); +86-10-8299-8532 (S.H.)

Academic Editor: Kewen Li
Received: 30 July 2016; Accepted: 31 August 2016; Published: 1 October 2016

Abstract: Development and utilization of deep geothermal resources, especially a hot dry rock (HDR) geothermal resource, is beneficial for both economic and environmental consideration in oilfields. This study used data from multiple sources to assess the geothermal energy resource in the Daqing Oilfield. The temperature logs in boreholes (both shallow water wells and deep boreholes) and the drilling stem test temperature were used to create isothermal maps in depths. Upon the temperature field and thermophysical parameters of strata, the heat content was calculated by 1 km × 1 km × 0.1 km cells. The result shows that in the southeastern part of Daqing Oilfield, the temperature can reach 150 °C at a depth of 3 km. The heat content within 3–5 km is 24.28 × 10^{21} J, wherein 68.2% exceeded 150 °C. If the recovery factor was given by 2% and the lower limit of temperature was set to be 150 °C, the most conservative estimate for recoverable HDR geothermal resource was 0.33 × 10^{21} J. The uncertainties of the estimation are mainly contributed to by the temperature extrapolation and the physical parameter selections.

Keywords: hot dry rock; temperature; resource base; Daqing Oilfield

1. Introduction

Geothermal energy coexisting with oil and gas started to be utilized, initially for house warming and vegetable greenhouse, in the early 1970s in the Huabei Oilfield [1–3]. Since 2000, oilfields of Daqing, Shengli, and Liaohe have also put efforts into geothermal energy utilization, and even further, attempted to produce electricity by low–medium temperature fluids (with the temperature lower than 150 °C) [4,5]. Recently, the development of enhanced geothermal system (EGS) technology has extended to the realm of geothermal resources, e.g., hot dry rock (HDR) geothermal resource. The main benefits to developing HDR in oilfields are that utilization of HDR is already largely in place and little additional investment is required [6–9]. Because of this reduced exploration and drilling cost, development of HDR geothermal energy in oilfields can become cost competitive.

Daqing Oilfield, in Heilongjiang Province, northeast China, had already produced a total of 1.95 billion tons of oil by 2007 as the largest oilfield of China, with a high and stable yield of around 50 million tons per annum from 1976 to 1997 [10]. However, the production has been decreasing since 1997. The annual production declined from the peak production of 56.0 million tons in 1997 to 41.6 million tons in 2007—an average decline rate of 2.9% per year. Höök et al. [10] predicted the future oil production in Daqing Oilfield will continue to decline, from 41.6 million tons in 2007 to

8.0 million tons in 2060. However, in contrast to the continuous reduction of the oil production, the water production has increased since 1996 and has sustained a high level since 2001 [11]. That will be difficult and challenging for the Daqing Oilfield with an average workforce of 250,000, especially under the background of sustainable lower oil price and increasingly stringent environmental requirements.

To cope with the crisis, the management of the Daqing Oilfield has been very much aware of the importance to build a green oilfield, which keeps a balance in the relationship resource exploitation and environmental protection in the oilfield. Geothermal energy is exactly what the management can choose for fulfilling the goal. Besides, the Daqing Oilfield is extremely abundant in medium to high enthalpy geothermal resources. The Daqing Oilfield is located in the northern part of the central Songliao basin, and beneath it a mantle pillow has developed due to upwelling of the upper mantle [12,13]. The region became a hot spot in the crust with high geothermal gradients, with an average value of 38.7 °C·km^{-1} [14]. The development of geothermal resources in the oilfield owns unique advantages, both at the stages of exploration and development.

A series of drilling stem test (DST) temperatures in Daqing Oilfield was published and a contour map of the average geothermal gradient was generated [15–17]. Liu et al. [18] compiled and investigated all these data and updated the isothermal map of the Daqing Oilfield. However, all previous studies were focused at the depths between 0 and 3 km. As the gradient strongly steepens at greater depths, as determined by the thermal conductivity of strata, using the average gradient extrapolated to the deeper temperature may cause great errors.

In this study, geothermal resource assessments were conducted within the northern central depression of the Songliao basin (Figure 1), where most of the oil drillings were located. The new continuous equilibrium temperature logs were created, incorporating DST temperature data collected in the Daqing Oilfield; distribution of temperature from 3 to 5 km was established; and the total geothermal resource at depths from 3 to 5 km with temperature exceeding 150 °C was assessed. Finally, herein uncertainty analysis and suggestions for exploration of geothermal energy on the oilfield are proposed.

2. Data Source

On Daqing Oilfield large amounts of wells have been drilled, and high-quality DST temperature data has been collected from a portion of the wells. Meanwhile, a fair number of wells have non-equilibrium bottom hole temperature (BHT) measurements. However, for commercial and security reasons, obtaining these temperatures is not easy. In this study, two types of temperature data were used: (1) high-precision temperature logs; and (2) DST temperatures, a tool left stationary for a period of time that collects formation fluid flowing from the well wall and gives the most accurate measurement of down-hole formation temperature shortly after drilling [19].

High-resolution continuous temperature logs were obtained from 25 shallow water wells (coded as WW1–WW25 in Figure 1) and 3 deep geothermal wells (coded as SK-2, W01, and W02 in Figure 1). The borehole temperature was measured using a cable system, which consists of a 42.9 mm diameter platinum sensor and a 5000 m long cable. The system allows temperature recording to a sensitivity of 0.01 °C, at a limiting accuracy of 0.1 °C. During the measurements, the downward speed was set at 6.5 m·min^{-1} and temperature data was recorded in the water-filled boreholes [20].

A total of 55 DST data from 25 oil wells were collected, which are shown in Figure 1 as the red spots. The data published by Wu and Xie [15], Wang et al. [16], Zhao [21], and Zhu [17] were also included in this study, shown in Figure 1 as the dark spots. The well locations are even and dense enough on a planar distribution for a temperature field study. In total, temperature data from 66 wells were applied in the calculation of temperature distribution in the Daqing Oilfield.

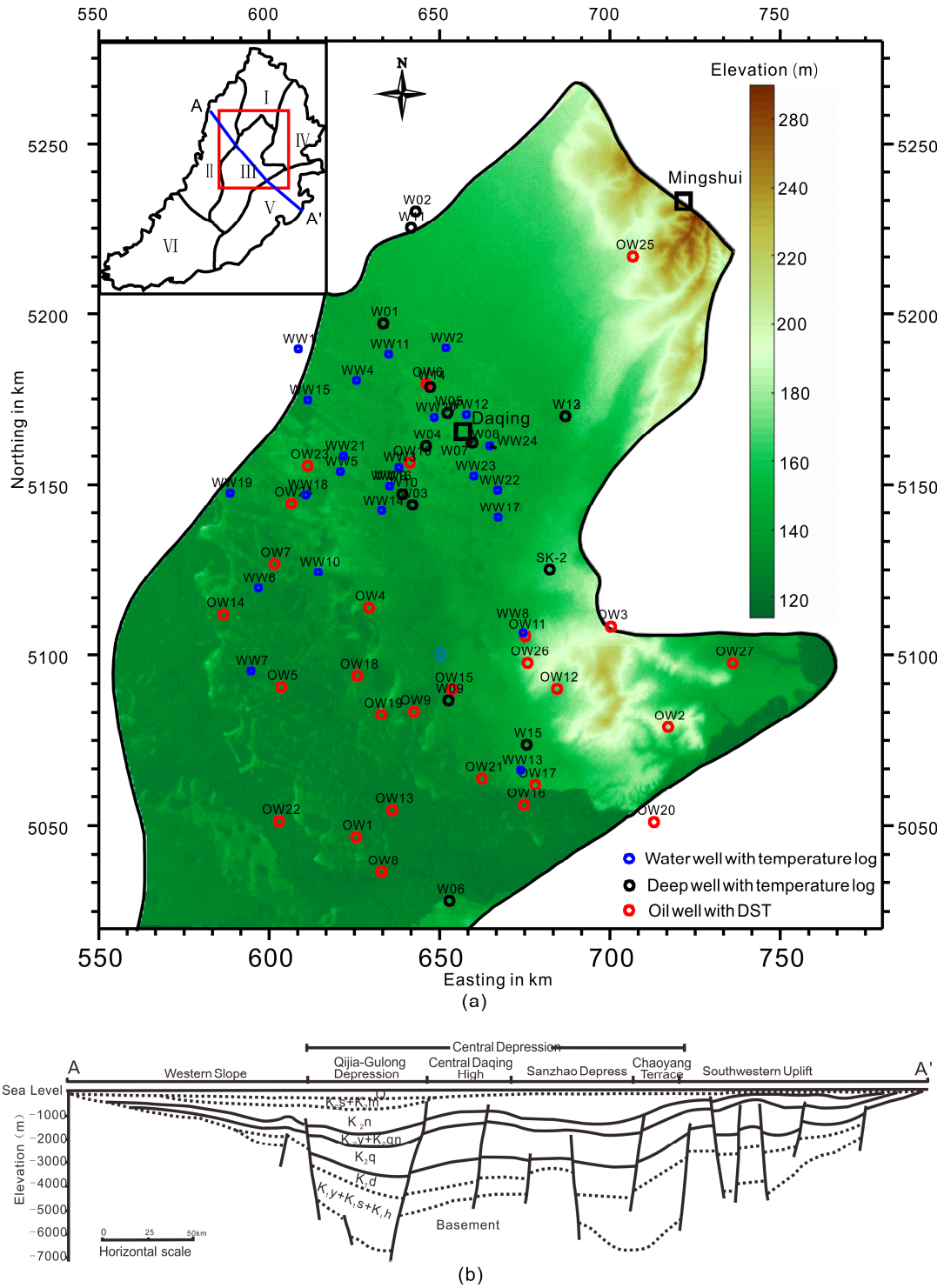

Figure 1. (**a**) The various temperature measurements on the Daqing Oilfield. Major structure zones in the Songliao basin and the structural location of the Daqing Oilfield are also shown; (**b**) stratigraphic cross-section of AA′, its location is shown in (**a**), interpreted with borehole-constrained seismic data. (Reproduced with permission from [22] Ryder et al., 2003 and [23] Wang et al., 2016). Formation symbols: K_1h is Huoshiling, K_1s is Shahezi, K_1y is Yingcheng, K_1d is Denglouku, K_2q is Quantou, K_2qn is Qingshankou, K_2y is Yaojia, K_2n is Nenjiang, K_2s is Sifangtai, K_2m is Mingshui. Tectonic units: I is North Slope, II is West Slope, III is Central Depression, IV is Southeast Uplift, V is North Uplift, VI is Southwest Uplift.

The temperature logs are shown in Figure 2. The temperature increases linearly with depth on the temperature–depth profiles of the deep wells, which represents a typical conductive temperature log. While a portion of shallow water wells exhibit a convective-type temperature log, on which temperature rapidly increases or decreases in local-depth intervals. These convective temperature logs were excluded from temperature extrapolation due to the distribution of groundwater activities. Thus, the occurrences of groundwater activities have been removed from the analysis, and conductive profiles will be only depending on the physical properties of the geological units. The temperature log of well SK-2 gives a precise temperature profile of the central depression with a depth of more than 4000 m.

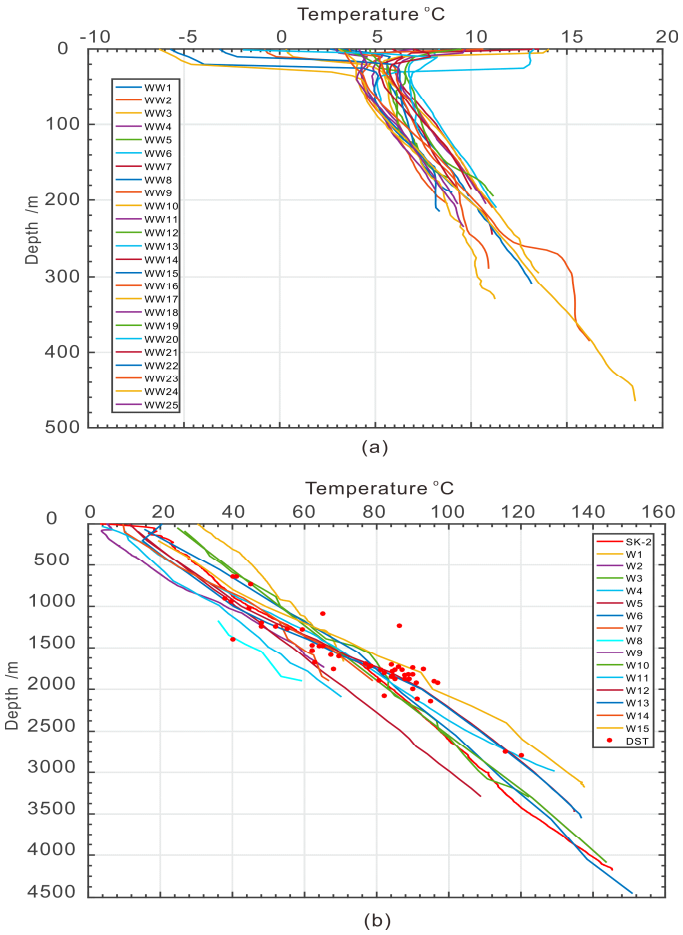

Figure 2. (**a**) Temperature logs from shallow water wells; (**b**) temperature logs from deep oil wells and geothermal wells, along with DST in the oil wells. Temperature logs of SK-2, W1, and W2 were newly measured in this study. W3–W6 are from Zhu [17], W7 and W8 are from Zhao [21], W9 and W10 are from Wu and Xie [15] and Liu et al. [18], and W11–W15 were extracted from oil test report.

The study area—in the northern part of the central depression zone in Songliao basin—is where the subsidence and depositional center of the basin is located (Figure 1). The thickness of the sedimentary layer is over 7 km. The cross-sections in west–east direction and north–south direction of the study area are shown in Figure 1a [24]. The regional strata mainly consist of the late Jurassic to Neogene (N) sedimentary layers: Huoshiling (K_1h), Shahezi (K_1s), Yingcheng (K_1y), Denglouku (K_1d), Quantou (K_2q), Qingshankou (K_2qn), Yaojia (K_2y), Nenjiang (K_2n), Sifangtai (K_2s), and Mingshui (K_2m) formations, and Quaternary (Q), in ascending order [25,26]. The main strata developed at the depth of 3–5 km are K_1h, K_1s, K_1y, and K_2q. The depth of the basement is shallower than 4 km underlying the Central Daqing High and the Sanzhao Depression.

3. Methodology

3.1. Temperature Extrapolation

The temperature data were measured at various depth from well to well, but 2000 m was the depth where a mass of measurements were concentrated. As the temperature measured at depths greater than 3 km is scattered and uneven, extrapolation of the temperature in a vertical direction is essential for investigation of deep geothermal resources. If the basic parameters (thermal conductivity and radiogenic heat production of different strata) were sufficient, the one-dimensional thermal conductive approaches could be used for extrapolating the temperature to greater depths [27,28]. Unfortunately, the Daqing Oilfield does not have enough thermal–physical parameters for this calculation. Besides, the geothermal gradient is depth-dependent in the Songliao basin [8]. Thus, the deep temperature cannot simply be extrapolated according to the geothermal gradient measured in the shallow wells.

Temperature gradient in the boreholes with continuous temperature log or more than two DST data points was calculated using linear least squares regression [29]. When only one DST data point was obtained, the gradient was calculated by:

$$G = (T - T_0)/(Z - Z_0), \quad (1)$$

The T_0 is given by 0.8–5 °C, the Z_0 is given by 30 m [17].

Above 2000 m, the temperature gradients in the shallow wells (depth less than 500 m) were obviously gentler than those in the deep wells (average depth greater than 1500 m). In general, the temperature gradient steepened when the depths increased to 2000 m (Figure 3). The difference can be considered as a systematic deviation of temperature gradient calculated from the measurements in shallow wells. The temperature gradients then were multiplied by a correction factor, which is determined by the ratio of average gradient of deep oil wells to average gradient of the water wells, to correct the gradients of water wells at the depth of 2000 m. It is notable that points with values higher than 45 °C/km mainly represent the gradients calculated from DST data, which reflect true condition of the strata more accurately. The effect of local climate on shallow water wells is another potential factor responsible for the discrepancy between gradients.

Beneath 2000 m, the temperature gradients were extrapolated using steady-state heat conduction equation. In the simple situation of steady-state (the radiogenic heat production was ignored) heat flow in the layer i and j can be expressed as [30]:

$$q_i = K_i \times G_i, \quad (2)$$

$$q_j = K_j \times G_j, \quad (3)$$

where q, G, and K represent the conductive heat flow, thermal gradient, and thermal conductivity of layer i and j, respectively. In the sedimentary layers with thickness less than 5 km, the heat-flow contribution of the radiogenic heat production will be less than 8 $mW \cdot m^{-2}$ [15], which could be ignored when compared with the average surface heat-flow values of 79 $mW \cdot m^{-2}$ in the Daqing Oilfield [17]. This allows the heat-flow values at various depths of a well to be considered as a constant number. The reverse relationship between thermal gradient and thermal conductivity can be derived from the Equations (1) and (2):

$$K_i/K_j = G_j/G_i, \quad (4)$$

Equation (4) means that the deep temperature gradient can be extrapolated just according to the thermal conductivity of various layers. Compared with the common 1-D steady-state heat conduction method, the radiogenic heat production was ignored. At the central depression zone, lateral variation of thermal conductivity is not as significant as it is in the vertical direction [31,32]. The thermal conductivity of different depth ranges was given according to Zhang et al. [8] and Wu [33].

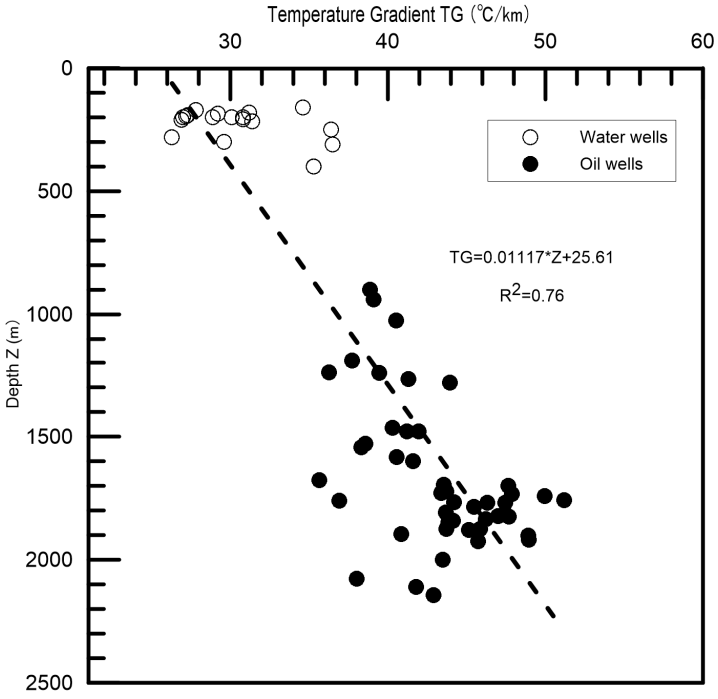

Figure 3. The relationship between the temperature gradient (TG) and depth.

Based on the calculated geothermal gradient, one-dimensional extrapolations were applied to estimate the temperature at 5 km depth in each well of the oilfield. Three scenarios were considered separately [34]: (1) when the temperature was measured at a depth greater than 5 km, the temperature is determined by straight-line interpolation between the BHT and the surface temperature; (2) when the temperature's measured depth was shallow than 5 km, the temperature of the upper layers was estimated according to (1) and the temperature at the lower layers was extrapolated from the bottom hole temperature with the equation:

$$Tz = T_1 + (Z - Z_1) \times G_z, \tag{5}$$

where Z and Z_1 are the depth of known and calculated temperature, respectively, T_z and T_1 are the known and calculated temperature, and G_z is the temperature gradient of the interval depth.

The calculation of deep temperature from the geothermal gradient values is different from common methods used by Blackwell et al. [35], Wang et al. [36], and other researchers. The computing process has not considered the radiogenic heat production within 5 km. The results might be slightly higher than actual values, but it is still acceptable since we have seriously considered the decreasing trend of temperature gradient and the actual measurements to corroborate the calculated values within the depths of 4 km, despite the fact that extrapolated depths are limited. The great benefit for this method is that relatively small amounts of data are required for calculation.

The temperature is obtained with the premise of a one-dimensional vertical steady-state, and it represents a steady-state temperature conduction field. Geological processes, including regional groundwater activities, rapid uplift, and erosion of the surface could make the temperature field deviate from the steady conduction dominated temperature field [37]. Furthermore, one-dimensional calculations of deep temperatures cannot reflect the lateral heat transfer in the rock contact zone with different heat conduction rates (uplift and depression contact zone) [38]. The above two factors may cause a significant difference between the calculated temperature and the real temperature, especially in the shallow depth. Thus, in the process of calculation, the convection-dominated temperature logs

were excluded. The dense and even distribution of temperature measurements facilitates a detailed and precise estimation of the lateral temperature variations.

3.2. Volumetric Method

The volumetric method is widely used on assessment of geothermal resources in oil and gas reservoirs. It refers to the calculation of thermal energy in the rock and the fluid that could be extracted based on specified reservoir volume, reservoir temperature, and reference or final temperature. However, it was found that the existing volumetric method tends to overestimate the geothermal reserves in oil and gas reservoirs. Thus the effects of oil and gas saturations on the estimation of geothermal reserve in oil and gas reservoirs are necessarily considered [39].

The heat in situ consists of the heat stored both in the rock skeletons and in the fluid of pores (either water or oil). If the porosity and permeability are extremely low, the heat stored in the fluid in pores is ignorable, the heat will just be stored in HDR, which can be exploited with EGS. The geothermal resource base is actually the heat content of the targeted medium calculated by Equation (6) [40,41]:

$$Q = \varrho \times Cp \times V \times (T - Tc) \quad (6)$$

where ϱ represents rock density, Cp represents rock specific heat, V is rock volume, T is rock temperature at a specific depth, and Tc refers to the average surface temperature or specific reference temperature. To calculate the heat in situ, the continental area of China was divided into 1 km × 1 km cells on the horizontal plane and 100 m slices in the vertical direction. The computational units can be considered as 1 km × 1 km × 0.1 km cuboids. For each cell, the parameters were given by the mean value. The total thermal energy Q for all systems (that is, the total mean identified accessible resource base) is simply the sum of the mean thermal energies of the individual systems. All the parameters are listed in the Table 1.

Table 1. Hot dry rock (HDR) resource reserves assessment and values of main parameters (Zhang et al. [8] and Wu [33]).

Depth Z (km)	Lithology	Thermal Conductivity K (W/K/m)	Density ϱ (g/cm^3)	Specific Heat C_p (J/kg/k)
2–3	Mudstone and Sandstone	2.31	-	-
3–4	Mudstone and Sandstone	2.51	2.47–2.61	940
4–5	Rhyolite and Tuffaceous breccia lava	2.87	2.70–2.80	1070

The volumetric method has been widely used in the HDR geothermal resource assessment due to its simplicity and availability. Utilization of the method in the oil and gas reserve need to be modified [42]. For the HDR resource from 3 to 5 km, because of the large resource base and relative low porosity, the effects of oil and gas saturation on the geothermal resource can be ignored.

4. Results

4.1. The Temperature Field

According to the temperature measurements at the depths from 3 to 5 km, the values ranged from 100 to 245 °C. The high temperatures are mainly distributed in the southeastern and central areas (i.e., Central Daqing High and Chaoyang Terrence), while the low temperature areas are localized in the northwestern part (i.e., Qijia-Gulong Depression). In general, from south to north and southeast to the northwest, temperature represents a gradual decrement trend (Figure 4). The discrepancy in temperature is proximately 40 °C at the depth of 3 km and increases to 80 °C at the depth of 5 km. The horizontal difference is contributed to by the relief of basement [15]. The detailed temperature distributions at depths are described below.

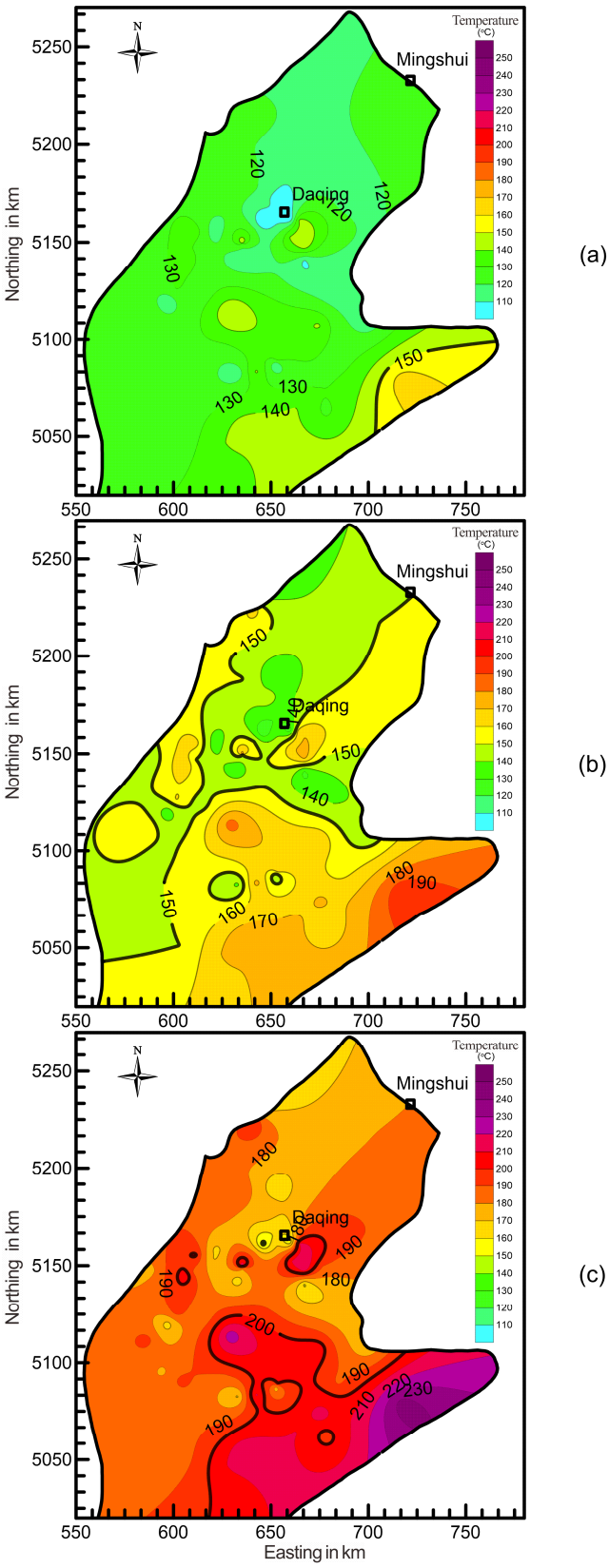

Figure 4. The temperature distribution at the different depth of 3 km (**a**), 4 km (**b**), and 5 km (**c**). The thick black lines show the isotherm of 150 °C and 200 °C.

(1) At the depth of 3 km, temperature ranges from 100 to 165 °C, showing the overall trend of being higher in the southeast and lower to the north and northwest (Figure 4a). The regions with temperatures higher than 150 °C are limited within Chaoyang Terrace, with area approximately 40 km^2. Temperature is low at the northern part of study area, especially in the Central Daqing High.

(2) At the depth of 4 km, temperatures are 121–199 °C, with the overall trend of being higher in the south and lower to the north (Figure 4b). The temperature at Chaoyang Terrace is as high as 190 °C. The total area with temperature exceeding 150 °C is about 850 km^2, which means approximate a half of the areas met the conditions. Low temperature area lies within the north of study area.

(3) At the depth of 5 km, temperatures are 147–245 °C, with the overall trend being same to the depth of 4 km (Figure 4c). Total area of the region with temperature higher than 200 °C reached 250 km^2, and mainly underlies Chaoyang Terrace, Sanzhao Depression, and Central Daqing High. Low temperature is exhibited at Qijia-Gulong Depression.

4.2. The Heat Content from 3 to 5 km

If hot dry rock is defined as the rocks in excess of 150 °C, then in other words, 150 °C is set as the lower boundary of temperature for the HDR geothermal resource [43,44]. The HDR geothermal resource is widely but unevenly developed at a great depth in the study area. The majority of the resource underlies the central part, southern part, and southeastern part of the area, at where the isotherm of 150 °C is shallower than 5 km. The shallowest depth of 150 °C isotherm is 3 km at Chaoyang Terrace. In consideration of the limitation of current drilling technology and economic condition, the study focused on the depths shallower than 5 km. At the range of depth from 3 to 5 km, HDR geothermal resources mainly exist in the central, southern, and southeastern parts of the study area.

In order to ascertain the geothermal resources reserves in Daqing Oilfield, volume method is used to assess the thermal energy. Results show that the total thermal energy from 3 to 5 km is 24.28 $\times$ 10^{21} J, wherein 68.2% (16.56 $\times$ 10^{21}) exceeds 150 °C (Table 2). Considering the limitations of economics and technology, the resource within depths from 3 to 5 km, accompanied by an expected temperature of 150–250 °C, can be developed as an HDR geothermal resource. If the conservative recovery factor of 2% is adopted to compute the recoverable energy, according by Sanyal [45], the limited recoverable resource at this depth is 0.33 $\times$ 10^{21} J, which is equivalent to 1.330 $\times$ 10^{13} t standard coal (Note: 1 standard coal is equivalent to 2.930760 $\times$ 10^7 J). Herein the recovery factor of 2% is a conservative estimate to the HDR resource from 3 to 5 km. The anticipated factor can be significantly higher than 2%. Thus, the midrange recoverable factor of 20% is more reasonable. That is to say, the recoverable resource is 10 times than the value above.

Table 2. Heat content in the Daqing Oilfield.

Depth Range (km)	$Q \times 10^{21}$ (J)				
	–150 °C	**150–180 °C**	**180–200 °C**	**200– °C**	**Total**
3.0–3.5	3.97	0.61	0.00	0.00	4.58
3.5–4.0	3.14	1.79	0.15	0.00	5.07
4.0–4.5	0.61	5.08	1.06	0.18	6.93
4.5–5.0	0.01	4.12	2.28	1.29	7.70
Total	7.72	11.60	3.50	1.46	24.28

Judging from the temperature of HDR resources at depths of 3–5 km, the HDR geothermal resource with the temperature lower than 150 °C is 7.72 $\times$ 10^{21} J, accounting for 31.8% of the total resource; the HDR geothermal resource with the temperature of 150–180 °C is 11.60 $\times$ 10^{21} J, accounting

for 47.8% of the total resource; the HDR geothermal resource with the temperature of 180–200 °C is 3.50 × 10^{21} J, accounting for 14.4% of the total resource; the HDR geothermal resource exceeding 200 °C is 1.46 × 10^{21} J, accounting for 6.0% of the total HDR resource. Approximately half the resource lies within the temperature range of 150–180 °C.

The resource bases at different depth intervals (0.5 km thick each), are shown in Figure 5. As the temperature increases with depth, the amount of resources is proportionate to the depth. At the depth ranges of 3.0–3.5 km, the temperature of the geothermal resource is up to 180 °C. The resource with temperature ranging from 180 to 200 °C appeared at the depth interval of 3.5–4.0 km. The resource with temperature above 250 °C makes up a small proportion (2.5%) at the depth of 4.0–4.5 km, and about 16.7% at the depth of 4.5–5.0 km.

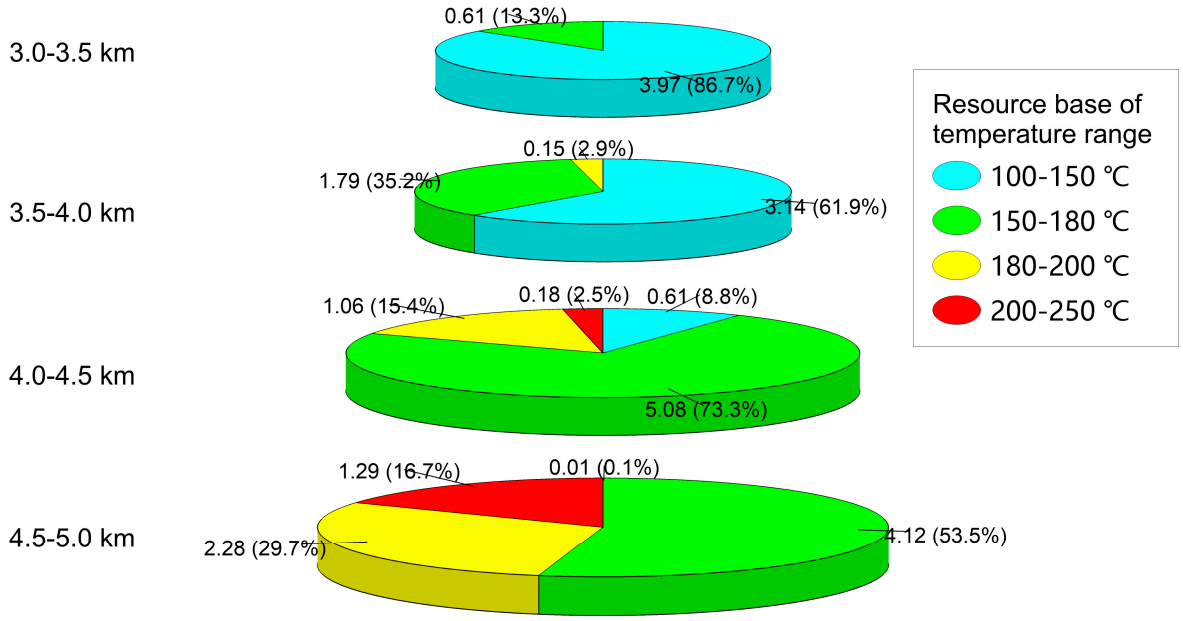

Figure 5. Heat content in place with various temperature ranges in the 0.5 km thick depth intervals from 3 to 5 km. The area of the pie represents the amount of the heat content. The number in front is the heat content in 10^{21} J, the number in the bracket is the percentage of the different temperature ranges in specific depth interval.

5. Discussion and Conclusions

As the deep strata are lacking in directly measured parameters (temperature, porosity, as well as strata division), the extrapolated parameters inevitably cause much uncertainty of the estimation of heat content in place. The uncertainty analysis of the heat content is to discuss the entire set of possible outcomes and the associated probabilities of occurrence [46]. The uncertainty of the estimation of heat content in place mainly depends on the calculated parameters, including the temperature, density, and porosity.

Due to the high geothermal potentials and low annual average temperature in the Daqing area, development and utilization of deep thermal energy has broad prospects in the Daqing Oilfield. In this study, we focused on the geothermal energy within the depth from 3 to 5 km with the temperature higher than 150 °C. For further recommendation, the basement rocks in this uplifted area could be reached at the depth less than 3 km, which is predicted to be fractured and exhibiting a certain level of permeability. For an economic operation, it is necessary to enhance the network of fractures by stimulation procedures to create a heat exchanger of adequate size. If only the geological conditions are considered, it is feasible to explore HDR geothermal resource in the Daqing Oilfield. This study

is focused on the assessment of a static resource base; the portions for economically viable power generation require further research. The contribution of this paper may be drawn as following:

(1) A total of 28 temperature logs were measured, and temperature data from 30 wells were collected, indicating that Daqing Oilfield was located in a geothermal anomalous area, with an average temperature gradient of 34 °C·km^{-1}.
(2) The median deep temperature field (3–5 km) was characterized according to the constraint of multiple-source temperature data.
(3) The heat content from 3 to 5 km is evaluated to be 24.28 × 10^{21} J. The limit of recoverable HDR resource at the depth interval is 0.33 × 10^{21} J, equivalent to 1.330 × 10^{13} t standard coal.

Acknowledgments: This research is supported by Sinopec Star Petroleum Ltd. (No. ZC06070007) and Sinopec Northeast Oilfield Company (No. ZC0607-0044). The temperature loggings were supported by China Geological Survey and Daqing Oilfield of CNPC.

Author Contributions: Yi Wang and Chao Zhang conceived and designed performed the experiments; Guangzheng Jiang, Shengbiao Hu, Yizuo Shi and Xiaoyin Tang analyzed the data and wrote the paper.

Conflicts of Interest: The authors declare no conflict of interest.

References

1. Zhang, L.; Yuan, J.; Liang, H.; Li, K. Energy from Abandoned oil and gas reservoirs. In Proceedings of the SPE Asia Pacific Oil and Gas Conference and Exhibition, Perth, Australia, 20–22 October 2008; Society of Petroleum Engineers: Richardson, TX, USA, 2008.
2. Xin, S.; Liang, H.; Hu, B.; Li, K. Electrical power generation from low temperature co-produced geothermal resources at Huabei oilfield. In Proceedings of the thirty-seventh Workshop on Geothermal Reservoir Engineering, Stanford, CA, USA, 30 January–1 February 2012. SGP-TR-194.
3. Wang, S.J.; Yan, J.H.; Li, M.; Li, K.W.; Hu, S.B. New advances in the study of oilfield geothermal resources evaluation. *Chin. J. Geol.* **2014**, *49*, 771–780. (In Chinese with English abstract)
4. Li, Q.; Yu, H.X. Geothermal power generation experiment engineering in buried-hill oilfield and its application prospect. *Chin. J. Geol.* **2012**, *32*, 20–23. (In Chinese with English abstract)
5. Li, K.W.; Wang, L.; Mao, X.P.; Liu, C.W.; Lu, J.H. Evaluation and efficient development of geothermal resource associated with oilfield. *Sci. Technol. Rev.* **2012**, *30*, 32–41. (In Chinese with English abstract)
6. Petty, S.; Bour, D.L.; Livesay, B.J.; Baria, R.; Adair, R. Synergies and opportunities between EGS development and oilfield drilling operations and producers. In Proceedings of the SPE Western Regional Meeting, San Jose, CA, USA, 24–26 March 2009; Society of Petroleum Engineers: Richardson, TX, USA, 2009.
7. Conser, A. Double Dipping: Utilizing Oil Wells for Geothermal Energy. *William Mary Environ. Law Policy Rev.* **2013**, *37*, 813–843.
8. Zhang, Y.; Li, Z.; Guo, L.; Gao, P.; Jin, X.; Xu, T. Electricity generation from enhanced geothermal systems by oilfield produced water circulating through reservoir stimulated by staged fracturing technology for horizontal wells: A case study in Xujiaweizi area in Daqing Oilfield, China. *Energy* **2014**, *78*, 788–805. [CrossRef]
9. Zhang, Y.; Li, Z.; Guo, L.; Gao, P.; Jin, X.; Xu, T. Feasibility Evaluation of EGS Project in the Xujiaweizi Area: Potential Site in Songliao Basin, Northeastern China. In Proceedings of the World Geothermal Congress, Melbourne, Australia, 19–25 April 2015; pp. 1–14.
10. Höök, M.; Tang, X.; Pang, X.; Aleklett, K. Development journey and outlook of Chinese giant oilfields. *Pet. Explor. Dev.* **2010**, *37*, 237–249. [CrossRef]
11. Zhai, Z.W.; Shi, S.M.; Zhu, H.L. Discussion on utilization of oilfield production water type geothermal resource-take Daqing Oilfield as an example. *J. Nat. Resour.* **2011**, *26*, 382–387.
12. He, C.; Dong, S.; Chen, X.; Santosh, M.; Niu, S. Seismic evidence for plume-induced rifting in the Songliao Basin of Northeast China. *Tectonophysics* **2014**, *627*, 171–181. [CrossRef]
13. Chen, L.; Tao, W.; Zhao, L.; Zheng, T. Distinct lateral variation of lithospheric thickness in the Northeastern North China Craton. *Earth Planet. Sci. Lett.* **2008**, *267*, 56–68. [CrossRef]
14. Tan, S.Y.; Shi, Y.Q.; Zhao, Y.J. The formation and prospective evaluation of geothermal resources in the Songliao Basin. *World Geol.* **2001**, *20*, 155–160. (In Chinese with English abstract)

15. Wu, Q.F.; Xie, Y.Z. Geothermal heat flow in the Songhuajiang-Liaoning Basin. *Seismol. Geol.* **1985**, *7*, 59–64. (In Chinese with English abstract)
16. Wang, J.; Huang, S.Y.; Huang, G.S.; Wang, J.Y. *Basic Characteristics of the Earth's Temperature Distribution in China*; Seismological Press: Beijing, China, 1990.
17. Zhu, H.L. Research on the Sedimentary Geothermal Resources in North Songliao Basin. Ph.D. Thesis, Northeast Petroleum University, Daqing, China, 2011. (In Chinese with English abstract).
18. Liu, C.; Li, K.; Chen, Y.; Chen, J. Geothermal Gradient in the Oilfields in China. In Proceedings of the 41st Workshop on Geothermal Reservoir Engineering, Stanford, CA, USA, 22–24 February 2016.
19. Beardsmore, G.R.; Cull, J.P. *Crustal Heat Flow: A guide to Measurement and Modelling*; Cambridge University Press: Cambridge, UK, 2001.
20. Jiang, G.; Tang, X.; Rao, S.; Gao, P.; Zhang, L.; Zhao, P.; Hu, S. High-quality heat flow determination from the crystalline basement of the south-east margin of North China Craton. *J. Asian Earth Sci.* **2016**, *118*, 1–10. [CrossRef]
21. Zhao, C.Q. Distribution Characteristics and the Resource Assessment of Geothermal Resources in Longfeng District. Ph.D. Thesis, Northeast Petroleum University, Daqing, China, 2012.
22. Ryder, R.T.; Jin, Q.; McCabe, P.J.; Nuccio, V.F.; Persits, F. *Qingshankou-Putaohua/Shaertu and Jurassic Coal-Denglouku/Nongan Total Petroleum Systems in the Songliao Basin, China*; US Geological Survey Bulletin 2203-A; US Geological Survey: Reston, VA, USA, 2003.
23. Wang, P.; Mattern, F.; Didenko, N.A.; Zhu, D.; Singer, B.; Sun, X. Tectonics and cycle system of the Cretaceous Songliao Basin: An inverted active continental margin basin. *Earth-Sci. Rev.* **2016**, *159*, 82–102. [CrossRef]
24. Sui, W.X. How to realize the geothermal resources: Exploration prospecting breakthrough and geothermal resource research in northern Songliao basin, Heilongjiang province. *Tectonophysics* **2013**, *606*, 1–13. (In Chinese with English abstract)
25. Feng, Z.Q.; Jia, C.Z.; Xie, X.N.; Zhang, S.; Feng, Z.H.; Cross, T.A. Tectonostratigraphic units and stratigraphic sequences of the nonmarine Songliao basin, northeast China. *Basin Res.* **2010**, *22*, 79–95.
26. Zhao, Z.; Xu, S.; Jiang, X.; Lin, C.; Cheng, H.; Cui, J.; Jia, L. Deep strata geologic structure and tight sandy conglomerate gas exploration in Songliao Basin, East China. *Pet. Explor. Dev.* **2016**, *43*, 13–25. [CrossRef]
27. Hurtig, E. Temperature and heat-flow density along European transcontinental profiles. *Tectonophysics* **1995**, *244*, 75–83. [CrossRef]
28. Tester, J.W.; Anderson, B.J.; Batchelor, A.S.; Blackwell, D.D.; DiPippo, R.; Drake, E.M.; Garnish, J.; Livesay, B.; Moore, M.C.; Nichols, K.; et al. *The Future of Geothermal Energy: Impact of Enhanced Geothermal Systems (EGS) on the United States in the 21st Century*; Massachusetts Institute of Technology: Cambridge, MA, USA, 2006; p. 372.
29. Haenel, R.; Stegena, L.; Rybach, L. *Handbook of Terrestrial Heat-Flow Density Determination: With Guidelines and Recommendations of the International Heat Flow Commission*; Springer Science & Business Media: Berlin, Germany, 2012.
30. Spichak, V.; Geiermann, J.; Zakharova, O.; Calcagno, P.; Genter, A.; Schill, E. Deep temperature extrapolation in the Soultz-sous-Forêts geothermal area using magnetotelluric data. In Proceedings of the 35th Workshop on Geothermal Reservoir Engineering, Stanford, CA, USA, 1–3 February 2010.
31. Nansheng, Q. Geothermal regime in the Qaidam basin, northeast Qinghai–Tibet Plateau. *Geol. Mag.* **2003**, *140*, 707–719. [CrossRef]
32. Rao, S.; Hu, S.B.; Zhu, C.Q.; Tang, X.Y.; Li, W.W.; Wang, J.Y. The characteristics of heat flow and lithospheric thermal structure in Junggar Basin, northwest China. *Chin. J. Geophys.* **2013**, *56*, 2760–2770. (In Chinese with English abstract)
33. Wu, X.X. Research of Geothermal Resources on Hot Dry Rock in North Songliao Basin. Ph.D. Thesis, Northeast Petroleum University, Daqing, China, 2014. (In Chinese with English abstract).
34. Chopra, P.; Holgate, F. A GIS analysis of temperature in the Australian crust. In Proceedings of the World Geothermal Congress, Antalya, Turkey, 24–29 April 2005.
35. Blackwell, D.D.; Negraru, P.T.; Richards, M.C. Assessment of the enhanced geothermal system resource base of the United States. *Nat. Resour. Res.* **2006**, *15*, 283–308. [CrossRef]
36. Wang, J.Y.; Hu, S.B.; Pang, Z.H.; He, L.J.; Zhao, P.; Rao, S.; Tang, X.Y.; Kong, Y.L.; Luo, L.; Li, W.W. Estimate of Geothermal Resources Potential for Hot Dry Rock in the Continental Area of China. *Sci. Technol. Rev.* **2012**, *30*, 25–31. (In Chinese with English abstract)

37. Hu, S.B.; Xiong, L.P. Correction for disturbance of vertical groundwater movement to heat flow measurement. *Chin. J. Geol.* **1994**, *29*, 85–92. (In Chinese with English abstract)
38. Xiong, L.P.; Gao, W.A. The characteristics of geo-temperature field in uplift and depression zone. *Chin. J. Geophys.* **1982**, *5*, 448–456. (In Chinese with English abstract)
39. Zhang, L.; Liu, M.; Li, K. Estimation of geothermal reserves in oil and gas reservoirs. In SPE Western Regional Meeting, San Jose, CA, USA, 24–26 March 2009; Society of Petroleum Engineers: Richardson, TX, USA, 2009.
40. Agemar, T.; Weber, J.; Schulz, R. Deep Geothermal Energy Production in Germany. *Energies* **2014**, *7*, 4397–4416. [CrossRef]
41. Muffler, L.J.P. *Assessment of Geothermal Resources of the United States, 1978*; Geological Survey: Reston, VA, USA, 1979.
42. Li, K.; Sun, W. Modified Method for Estimating Geothermal Resources in Oil and Gas Reservoirs. *Math. Geosci.* **2015**, *47*, 105–117. [CrossRef]
43. Olasolo, P.; Juárez, M.C.; Morales, M.P.; D'Amico, S.; Liarte, I.A. Enhanced geothermal systems (EGS): A review. *Renew. Sustain. Energy Rev.* **2016**, *56*, 133–144. [CrossRef]
44. Rybach, L.; Bodmer, P.; Pavoni, N.; Mueller, S. Siting Criteria for Heat Extraction from Hot Dry Rock—Application to Switzerland. *Pure Appl. Geophys.* **1978**, *116*, 1211–1224. [CrossRef]
45. Sanyal, S.K. Sustainability and renewability of geothermal power capacity. In Proceedings of the World Geothermal Congress, Antalya, Turkey, 24–29 April 2005.
46. Williams, C.F.; Reed, M.J.; Mariner, R.H. *A Review of Methods Applied by the US Geological Survey in the Assessment Of Identified Geothermal Resources*; US Geological Survey Open-File Report; US Geological Survey: Reston, VA, USA, 2008.